Arch. Metall. Mater. **70** (2025), 2, 633-638

DOI: https://doi.org/10.24425/amm.2025.153464

A. BREUS[1*], S. ABASHIN[1], O. SERDIUK[1]

ATMOSPHERIC ARC DISCHARGE AS A FABRICATION TOOL FOR SYNTHESIZING IRON NANOPARTICLES EMBEDDED INTO CARBON NANOSHEETS

Simple and reliable method was engaged to obtain densely-packed and easy-to-manipulate arrays of iron nanoparticles protected from the potential action of atmospheric factors, which are in demand for catalytic applications. For the purpose, atmospheric arc discharge was initiated in a discharge gap of 10 mm between stainless steel electrodes. The gap was filled with a mixture of micrometre-sized powders of graphite and iron. After passing a direct arc current of 140 A for 2 min, a significant change in the morphology and chemical composition of the initial materials was observed. After a positive polarity was supplied to a smaller electrode, carbon nanosheets with an average width of 200 mm and thickness of about 20 nm that host Fe nanoparticles with diameters mostly ranging from 10 to 40 nm were found. Moreover, the initial oxygen content of 18% wt. was reduced to just 4% wt., as measured in the synthesized nanocomposites.

Keywords: Arc Discharge; Carbon 2D Nanostructures; Iron Nanoparticles; Composite

1. Introduction

Carbon nanostructures and carbon-based nanocomposites are extensively studied for the past decade and are considered to be perspective materials for a wide range of applications, such as field emission, wearable electronics, energy storage [1], and hydrogen conversion [2]. Pure graphene materials and graphene-based composites exhibit different properties that complement each other, expanding their potential applications. Implementation of carbon and graphene nanomaterials in supercapacitors was reviewed by Yang et al. [3], while polymer and graphene nanocomposites allow significant improvement in mechanical properties in comparison with pure materials [4]. Moreover, the morphology of the materials plays also an important role, and the effects of transformation of material morphology from micro- to nanostructure has been investigated in metallurgy [5]. For example, carbon nanotubes were used to modify austenitic steels [6], while a comprehensive review of the growth strategies and properties of metal matrix nanocomposites describe the successful employment of both carbon nanotubes and nanosheets [7].

The introduction of metal nanoparticles and morphology of carbon interface are dependent on a particular application. Carbon matrix is considered to be remedy to protect nanosized metal oxide structures from negative effects caused by elevated temperatures [8]. To improve the efficiency of carbon nanostructure production technologies in terms of energy consumption and production rates, iron-catalysed graphitization was proposed by Hunter et al., when carbon precursors (amorphous carbon) undergo a reaction of pyrolysis at presence of iron catalyst (FeO_x nanoparticles) [9]. At that, the temperature of the process ranges from 600 to 1200°C, and the time of the synthesis is about of a few hours. Unfortunately, this simple approach results mostly in growth of carbon-shelled nanoparticles or nanotubes, while 2D interface with the embedded nanoparticles is considered to be the most perspective. Influence of morphology of metal catalyst to the morphology of generated carbon nanostructures was observed by Sharma et al. [10]. When changing the thickness of the deposited catalyst layer (Fe) from 5 nm to 10, 20, and 50 nm, an average size of Fe nanoparticles obtained after the treatment of the initial layer by use of microwave plasma enhanced CVD (MPECVD) was increased from 25 nm to 30, 80, and 180 nm, respectively. At that, the carbon nanostructures grown for 1.5 min on the catalyst at presence of acetylene, changed their morphology from curved carbon nanotubes (CNTs) to vertically aligned CNTs, noodles shaped CNTs, and, finally, graphene nanoflakes, thus showing a transition from 1D to 2D nanostructures. Influence of catalyst to the growth processes was also reported by Panahi et al. [11].

[1] NATIONAL AEROSPACE UNIVERSITY, KHARKIV 61070, UKRAINE

* Corresponding author: a.breus@khai.edu

Generally, fabrication methods greatly affect the final result with respect to the formation of a nanostructure with specified chemical composition and morphology. A lot of control parameters complicate the development of the most effective technology of synthesis [12], and the investigation of the effects caused by the controls to tune the morphology of even 2D vertical graphene show a complex set of equations [13], yet it is not simpler than a description of a process of synthesis of 1D nanowires [14]. The problem becomes more complicated, when metals are introduced into the process. A number of methods has been developed for the last decade to fabricate the carbon nanostructures and their composites, from thermal [15] to mechanical milling used for the preliminary stage of carbon powder preparation [16]. The majority of the techniques employ complex and expensive equipment, and often take a long time to complete the process. A reactor that incorporates a solid metal electrode covered with films of polyether ether ketone (PEEK) and Teflon insulators, completed with glycine used as liquid electrode, was employed to conduct synthesis of carbon-encapsulated TiO_2, Ag and Fe_3O_4 nanocomposites by pulsed arc discharged plasma (4 Hz) for about 80 min [17]. It was confirmed that the graphite shell prevents the agglomeration of the metal and metal oxide nanoparticles. Three-step electroless plating was applied to prepare nickel-coated graphite nanosheets to be further implemented for conducting networks [18].

Plasma has attracted a lot of attention as a production tool due to its high flexibility towards the energy and particle control [19], simplicity of the design of some rectors, which utilize glow discharge [20], as well as possibility of engagement of magnetic fields to conduct the smart control over the treatment fluxes [21]. In particular, a successful growth of carbon nanostructures in magnetron discharge was reported [22]. To synthesize carbon nanowalls, glow discharge was implemented by Bo et al. in a configuration of a multiple-pin cathode and a grounded anode (both made of stainless steel) separated by a gap of 5 and 10 mm from each other [23]. In the experiment, the anode was considered to be the growth substrate that was held at 700°C, and the discharge gap was filled with the mixture of CH_4 and Ar (1:9) bubbled through a deionized water. The time of growth was changed from 0.5 to 10 min. At that, the discharge voltage at about 2.8-3.3 kV and the current density of about 9 A/m^2 were sustained at atmospheric pressure. Unfortunately, the direct approach cannot often meet the requirements of high productivity and material purity. That is why rather expensive radiofrequency (RF) and microwave (MW) plasma sources are engaged to reach the aims. A successful implementation of capacitively couple radio-frequency plasma was reported by Liu et al. to grow carbon nanosheets in atmosphere of methane with addition of hydrogen (from 0 to 85%) at the temperature of 500°C for 1 h [24]. Glass samples with Ni, Ni/Co, Co/Ni and Ni/Zn magnetron-deposited thin films were used as the growth substrates. Both flat and standing nanosheets were observed in the experiment, and the presence of metal nanoparticles is not reported on them. A single-step process of synthesis of graphene nanostructures by utilization of microwave 2.45 MHz plasma was reported by Yeh et al. [25]. Methane-hydrogen gas mixture introduced into a chamber at a pressure of 10^{-3} – 10 Torr to conduct the synthesis of vertical graphene nanostructures with a typical height of a few mm. Moreover, microwave plasma was engaged for post-treatment of manganese-iron oxide nanoparticles to increase band gap energy and improve their crystallinity [26]. A high-productivity method of fabrication of graphene-like carbon reinforced copper matrix composites was proposed by Shu et al. by implementing an atmospheric plasma jet CVD, where a pulsed arc discharge serves as a production tool [27]. Atmospheric plasma processes are widely used for this purpose, and a comprehensive review was reported by Dato [28]. Low production rates of about 10^{-3} to 10^{-1} g/h are considered to be the main challenge at that. A combined plasma setup, which comprises a microwave and a capacitively coupled plasma setups, was implemented to obtain the well-defined and dense arrays of the vertically-aligned carbon nanowalls for the time of growth of 290 s at low pressure of 1 Pa and the substrate temperature of 650° [29]; however, the complexity of the setup increases the production cost. The expensiveness of the RF and MW equipment hinders the large-batch production, and urges to seek alternatives.

Arc discharge methods conducted by use of custom-designed or industrial equipment, are considered to be the alternative. DC arc was initiated between the graphite electrodes immersed into a chamber filled with helium at the pressure of 10^5 Pa; the anode was filled with powder composed of graphite, CuO and ZnO, and the discharge current of 120 or 150 A was applied to grow multi-layered graphene sheets on the cathode [30]. Pure graphite electrodes were engaged in DC arc setup, and the cathode was sharpened to hinder the formation of a deposit on the cathode while the anode was rectangular to increase the evaporation from the cathode [31]. The distance between the electrodes was 1 mm, and the gap was filled with helium at the pressure of 2650 Pa to sustain the arc at 30 V and 100 A of the discharge power for 2 min 30 s. It was found that spherical carbon nanoparticles and multi-walled carbon nanotubes were grown on the cathode while graphene nanoflakes were synthesized on the chamber walls, this urging to assume about the necessity of more 'mild' plasma conditions to obtain 2D carbon nanostructures. DC arc (60-80 A, 20-40 V, 30 s) in argon was implemented by Shen et al. to produce Fe nanoparticles encapsulated by carbon shell as thin as two atomic layers; however, the product was mostly presented by the separate nanostructures not incorporated into a formation like 2D nanosheet [32]. Toxic and hazardous gases were not implemented in the arc discharge process developed by Tan et al. [33]. To synthesize a multilayer graphene structure, argon atmosphere maintained at the gas pressure of 53.3 kPa served as the protection shield to conduct 35 A of the arc current between two graphite rods connected to the terminals of a welder power source. High yield of Fe nanoparticles encapsulated by carbon shell was observed by Zhang et al. after implementation of DC arc setup in atmosphere of nitrogen [34]. At that, the cathode was made of pure graphite, while the anode was made of iron oxide and graphite powders (9:1); the discharge current of 30-40 A was passed for 2 min to get the

nanostructures. Moreover, arc discharge was successfully implemented to improve absorption capability of graphene nanoflakes after doping the growing nanostructures with nitrogen atoms extracted from nitrogen plasma [35]. It clear that all cases should involve fitting of the processing chambers with a pump system to provide the creation of an atmosphere of different gases kept under a specified pressure, which increase the production cost and complicates the fabrication process. Even so, the vast range of arc-based technologies cannot meet the demands of modern science and industry, specifically concerning the generation of large yields of metal nanoparticles, packed into a flat graphite interface to prevent them from spraying during the production stage, and from oxidation – after the production. This paper outlines the creation of an atmospheric arc discharge technology for producing metal nanoparticles embedded in extensive carbon nanosheets.

2. Experimental

To synthesize the nanomaterials, industrial arc welder was engaged to conduct the process in atmospheric environment. A pallet made of AISI 304 stainless steel was used as a substrate to be filled with a graphite powder (disk-shaped microparticles with a diameter less than 200 mm and thickness less than 1 mm) containing 2.5% wt. of iron particles with a diameter less than 20 mm. Preliminary study by use of a scanning electron microscope (SEM) facility allowed determining the oxygen content of 18% wt. in the mixture. A disk-shaped (∅ 25 mm × 2 mm) stainless steel sample (AISI 304) was immersed into the graphite powder, and the distance of 10 mm between the sample and pallet surface was sustained. Welder tongs were connected to the sample and pallet. Then two sets of experiments were conducted with respect to DC polarity supplied to the tongs: (i) negative and positive polarities were supplied to the sample and pallet, respectively, and (ii) the polarities were interchanged (Fig. 1). In both sets of experiments DC arc of 140 A was passed through the graphite powder for 2 min. The described parameters correspond to the typical values found in the above-cited literature for the arc-based technology. In both cases, sparking was observed in the gap, while there were no obvious signs of heating of the powder or sample.

After the experimental runs, the samples were extracted from the powder; a black deposit was formed on the parts of the samples immersed into the powder. The samples were transferred to a preparatory table where they were cooled in atmosphere; at that, a graphitic deposit formed on the samples was partially removed because of the cooling. Then, the samples with the carbon layer, and the fallen deposit were subjected to scanning electron microscopy (SEM) and transmission electron microscopy (TEM).

3. Results and discussion

For the samples treated at negative polarity of DC current supplied through the tongs, typical SEM images of the deposit found of the sample surface are shown in Fig. 2. General view of the structures found on the sample, is shown in Fig. 2(a), while the magnified view shown in Fig. 2(b) reveals a carbon deposit with iron microparticles embedded into it. At that, the fallen deposit also exhibits similar composition.

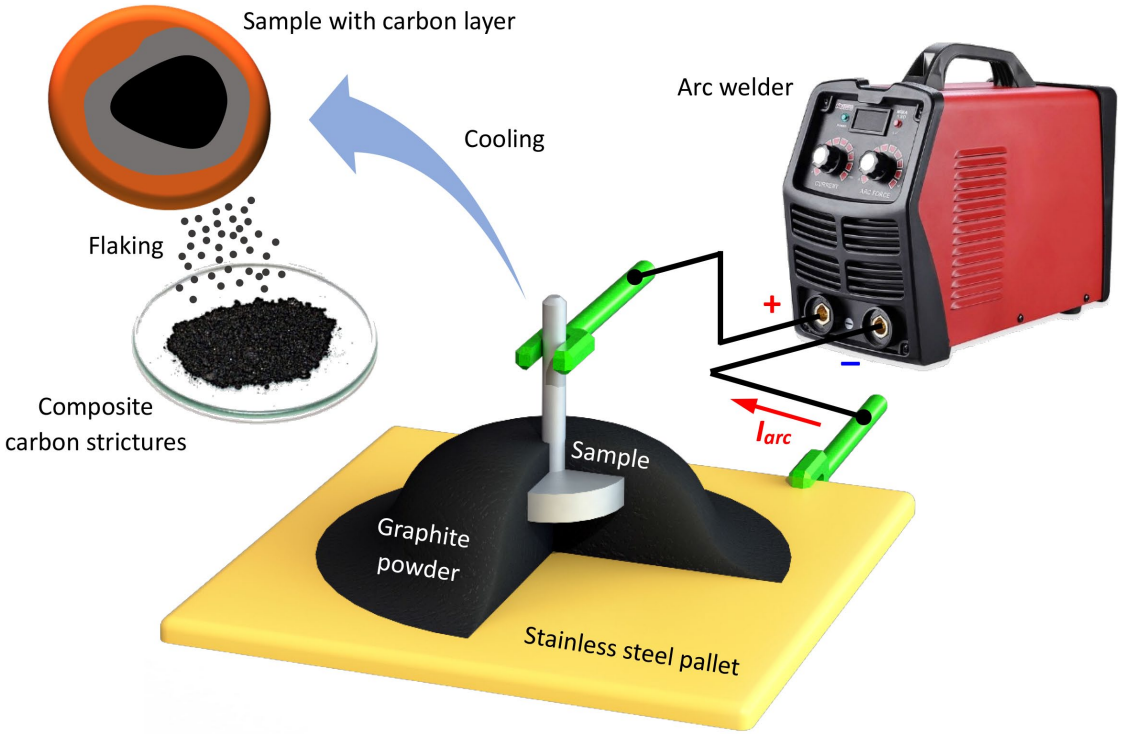

Fig. 1. A schematic of an experimental setup

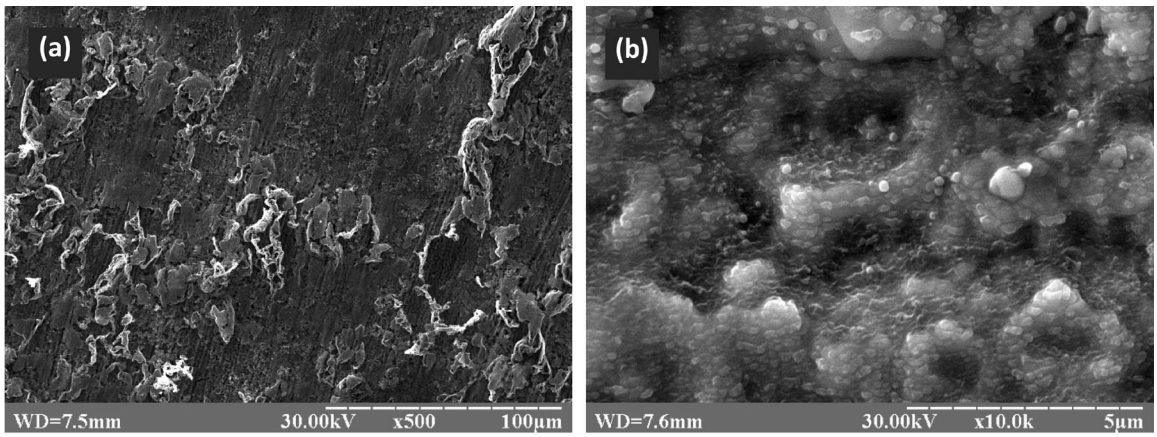

Fig. 2. SEM images of a sample used as a negatively biased electrode in atmospheric arc discharge setup with (a) general view of the film-like structures covering the sample and (b) magnified view revealing a carbon deposit with embedded iron microparticles

More interesting results were observed when positive polarity of DC arc was applied to the sample while the negative polarity was delivered to the pallet. General view of the sample surface is shown in Fig. 3(a), and extended (up to 200 mm in width) 2D microstructures can be distinguished on the surface. Concordance of the size with the sizes of the graphitic powder allows suggesting that the microparticles are just the attached elements of the powder. At that, the general view reveals rather dense structure of the film on the copper sample, which is similar to the observed in the first set of experiments. However, the same 2D microstructures shown in Fig. 3(b) are observed as separate sheets of high transparency in SEM processing tool. At the same time, the study conducted for the fallen deposit, revealed the folded 2D graphitic sheets shown in Fig. 3(c), and the nanometre-size thickness of the sheet of 18.5 nm was measured, as it is shown in Fig. 3(d). Thus, the application of DC arc discharge, when the negative polarity is supplied to the pallet containing the powder, allows generating 2D nanosheets, which are well-defined with small number of wrinkles, unlike the typical 2D nanostructures in the cited literature. It should

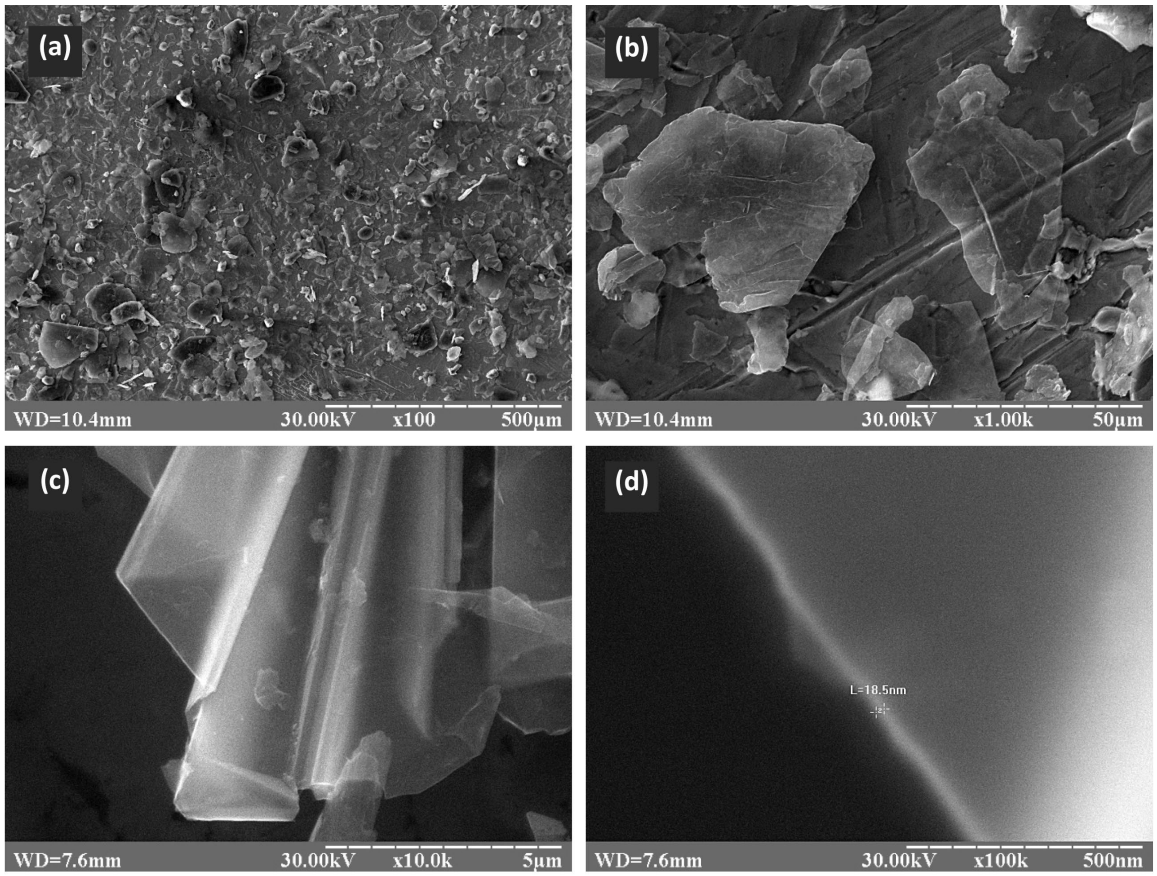

Fig. 3. SEM images (a) of a sample used as a positively biased electrode in atmospheric arc discharge setup, (b) graphite nanoflakes grown on the sample, (c) folded graphite nanosheet found in the deposit fallen from the sample during the cooling, (d) thickness of the nanosheet of 18.5 nm

be mentioned that the resolution of SEM is lower than that of TEM, and the dimensional accuracy is correspondingly lower; however, in this case the relative measurement error was not exceeding of 5%.

EDS analysis confirmed small amount of oxygen (4% wt.) in the graphitic structure, which is, however, much less than the initial oxygen content (18% wt.) in the powder. The elemental composition was determined using an XR-100SDD spectrometer (Amptek, USA). The resolution on the Mn Kα line was 125 eV, and the relative error in measuring the mass fraction of the element did not exceed: 4% – for elements with a mass fraction of more than 10%; 20% – for elements with a mass fraction range from 1% to 10%: 50% – for elements with a mass fraction range from 0.1% to 1%. The elemental composition was measured at ten points and then averaged.

Both of the nanosheets from the sample surface and fallen deposit were exposed to TEM study with a purpose of investigation of their structure, and the results are shown in Fig. 4(a) and Fig. 4(b), respectively. The substructures of both formations are similar, and composed of the graphitic sheets that incorporate iron nanoparticles with diameters ranged from 10 to 200 nm. Moreover, the observation of the nanosheet edges reveals another feature of the structure, namely, thin layer of graphite that envelops the nanoparticles and may serve as a protection layer that prevents the nanoparticles from oxidation. A magnified view shown in Fig. 4(d) allows to conclude the relatively narrow distribution of the iron nanoparticles on their sizes, since most of them are characterized with diameters of 10 to 40 nm.

4. Conclusions

Atmospheric arc discharge ignited in a mixture of graphite powder with a small amount of iron microparticles has proved to be a useful tool to fabricate a large yield of iron nanoparticles embedded into graphitic nanosheets. To conduct the process a positively-biased sample was immersed into the powder that was put onto a negatively-biased stainless-steel pallet. After passing the arc current between the electrodes, since morphology as chemical composition of the components of the initial mixture was significantly changed. Separate micrometre sized graphite (~200 mm × 1 mm) and iron particles (~20 mm) were transformed into the graphite sheets of approximately the same width but of a nanometre thickness (of about 20 nm), with a number of Fe nanoparticles (~10 to 40 nm) incorporated into the nanosheets. The proposed technique can be useful for the development of highly-productive, cheap, and reliable technology of mass production of catalytic Fe nanoparticles protected from the oxidation by the graphitic shell. Future studies are planned to develop the presented solution in terms of precise

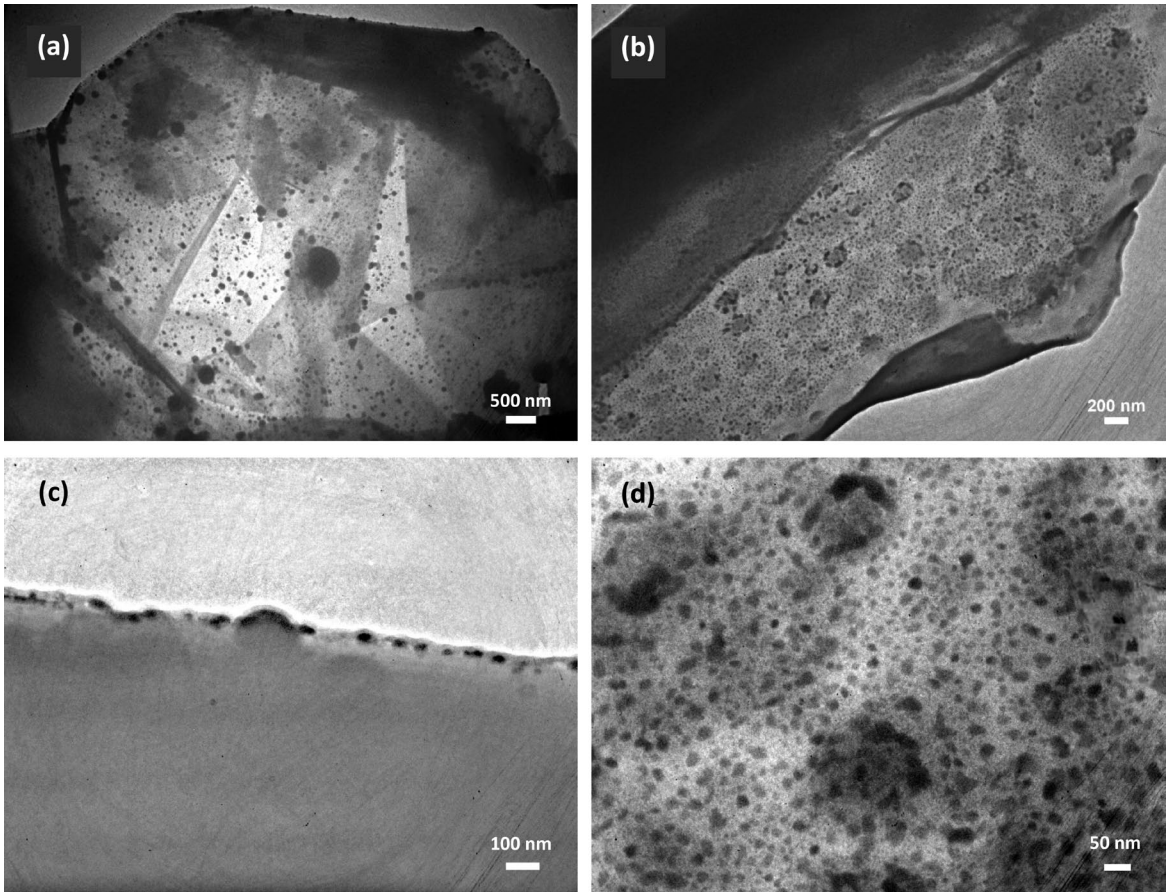

Fig. 4. TEM images of (a) the nanosheet from the sample surface, (b) nanosheet found in the fallen deposit, (c) edge of the nanosheet where iron nanoparticles are embedded into the graphite layer, (d) dense array of iron nanoparticles with diameters from 10 to 200 nm embedded into the graphite nanosheet

characterization of structure and chemical composition, as well as homogeneity of the produced material and practical applications.

Acknowledgments

The authors acknowledge the support from the project financed by the National Research Foundation of Ukraine, under grant agreement No. 2020.02/0119. A. Breus acknowledges the support from NATO Science for Peace and Security Programme under grant id. G5814 project NOOSE.

REFERENCES

[1] W. Zheng, X. Zhao, W. Fu, ACS Appl. Mater. Interfaces **13**, 9561-9579 (2021). DOI: https://doi.org/10.1021/acsami.0c19188

[2] V. Ruzaikin, I. Lukashov, Results Eng. **15**, 100600 (2022). DOI: https://doi.org/10.1016/j.rineng.2022.100600

[3] Z. Yang, J. Tian, Z. Yin, C. Cui, W. Qian, F. Wei, Carbon **141**, 467-480 (2019). DOI: https://doi.org/10.1016/j.carbon.2018.10.010

[4] R. Shah, A. Kausar, B. Muhammad, S. Shah, Polym. Plast. Technol. Eng. **54** (2), 173-183 (2015). DOI: https://doi.org/10.1080/03602559.2014.955202

[5] J. Jeon, S. Choi, N. Seo, Y.H. Moon, I.-J. Shon, S.-J. Lee, Arch. Metall. Mater. **65** (4), 1249-1254 (2020). DOI: https://doi.org/10.24425/amm.2020.133678

[6] J. Górka, T. Kik, M. Burda, Arch. Metall. Mater. **67** (1), 349-356 (2022). DOI: https://doi.org/10.24425/amm.2022.137765

[7] S.C. Tjong, Mater. Sci. Eng. R **74**, 281-350 (2013). DOI: http://dx.doi.org/10.1016/j.mser.2013.08.001

[8] P. Bijesh, V. Selvaraj, V. Andal, Mater. Today-Proc. **55**, 212-219 (2022). DOI: https://doi.org/10.1016/j.matpr.2021.06.163

[9] R.D. Hunter, J. Ramırez-Rico, Z. Schnepp, J. Mater. Chem. A **10**, 4489 (2022). DOI: https://doi.org/10.1039/D1TA09654K

[10] H. Sharma, A.K. Shukla, V.D. Vankar, Mater. Chem. Phys. **137**, 802-810 (2013). DOI: http://dx.doi.org/10.1016/j.matchemphys.2012.10.013

[11] A. Panahi, Z. Wei, G. Song, Y.A. Levendis, Ind. Eng. Chem. Res. **58**, 3009-3023 (2019). DOI: https://doi.org/10.1021/acs.iecr.8b05770

[12] M.M. Ramli, N.H. Osman, D. Darminto, M.M.A.B. Abdullah, Arch. Metall. Mater. **67** (3), 963-966 (2022). DOI: https://doi.org/10.24425/amm.2022.139689

[13] S. Alancherry, M.V. Jacob, K. Prasad, J. Joseph, O. Bazaka, R. Neupane, O.K. Varghes, O. Baranov, S. Xu, I. Levchenko, K. Bazaka, Carbon **159**, 668-685 (2020). DOI: https://doi.org/10.1016/j.carbon.2019.10.060

[14] O. Baranov, M. Košiček, G. Filipič, U. Cvelbar, Appl. Surf. Sci. **566**, 150619 (2021). DOI: https://doi.org/10.1016/j.apsusc.2021.150619

[15] M. Sabet, K. Mahdavi, F. Salmeh, Arch. Metall. Mater. **65** (2), 595-600 (2020). DOI: https://doi.org/10.24425/amm.2020.132797

[16] O. Gnytko, A. Kuznetsova, Arch. Mater. Sci. Eng. **113** (2), 69-76 (2022). DOI: https://doi.org/10.5604/01.3001.0015.7019

[17] Y. Lin, W. Zhu, R. Gou, H. Kita, X. Hu, L. Zhu, Wahyudiono, H. Kanda, M. Goto, J. Environ. Chem. Eng. **10**, 107771 (2022). DOI: https://doi.org/10.1016/j.jece.2022.107771

[18] Q. Li, G.-Z. Zeng, W.-F. Zhao, G.-H. Chen, Synthetic Met. **160**, 200-202 (2010). DOI: https://doi.org/10.1016/j.synthmet.2009.09.029

[19] O. Baranov, M. Romanov, Plasma Process. Polym. **6** (2), 95-100 (2009). DOI: https://doi.org/10.1002/ppap.200800131

[20] A. Breus, S. Abashin, I. Lukashov, O. Serdiuk, Arch. Mater. Sci. Eng. **114** (1), 24-33 (2022). DOI: https://doi.org/10.5604/01.3001.0015.9850

[21] O. Baranov, J. Fang, M. Keidar, X. Lu, U. Cvelbar, K.K. Ostrikov, IEEE Trans. Plasma Sci. **42** (10), 2464-2465 (2014). DOI: https://doi.org/10.1109/TPS.2014.2323263

[22] A. Breus, S. Abashin, O. Serdiuk, J. Achiev. Mater. Manuf. **109** (1), 17-25 (2021). DOI: https://doi.org/10.5604/01.3001.0015.5856

[23] Z. Bo, K. Yu, G. Lu, P. Wang, S. Mao, J. Chen, Carbon **49**, 1849-1858 (2011). DOI: http://dx.doi.org/10.1016/j.carbon.2011.01.007

[24] W. Liu, T. Dang, Z. Xiao, X. Li, C. Zhu, X. Wang, Carbon **49**, 884-889 (2011). DOI: http://dx.doi.org/10.1016/j.carbon.2010.10.049

[25] N.-C. Yeh, C.-C. Hsu, J. Bagley, W.-S. Tseng, Nanotechnology **30**, 162001 (2019). DOI: https://doi.org/10.1088/1361-6528/aafdbf

[26] M.A. Busharat, M.Y. Naz, S. Shukrullah, M. Zahid, Arch. Metall. Mater. **67** (3), 837-842 (2022). DOI: https://doi.org/10.24425/amm.2022.139673

[27] S. Shu, Q. Yuan, W. Dai, M. Wu, D. Dai, K. Yang, B. Wang, C.-T. Lin, T. Wuebben, J. Degenhardt, C. Regula, R. Wilken, N. Jiang, J. Ihde, Mater. Des. **203**, 109586 (2021). DOI: https://doi.org/10.1016/j.matdes.2021.109586

[28] A. Dato, J. Mater. Res. **34**, 214-230 (2019). DOI: https://doi.org/10.1557/jmr.2018.470

[29] T. Ichikawa, N. Shimizu, K. Ishikawa, M. Hiramatsu, M. Hori, Carbon **161**, 403-412 (2020). DOI: https://doi.org/10.1016/j.carbon.2020.01.064

[30] A. Kane, I. Hinkov, O. Brinza, M. Hosni, A.H. Barry, S.M. Cherif, S. Farhat, Coatings **10**, 308 (2020). DOI: http://dx.doi.org/10.3390/coatings10040308

[31] R. Kumar, R.K. Singh, P.K. Dubey, R.M. Yadav, D.P. Singh, R.S. Tiwari, O.N. Srivastava, J. Nanopart. Res. **17**, 24 (2015). DOI: https://doi.org/10.1007/s11051-014-2837-9

[32] C. Shen, Z. Lishuang, C. Lan, Z. Fan, L. Kui, J. Fengmin, L. Ling, S.A. Shah, Trans. Tianjin Univ. **21**, 011-018 (2015). DOI: https://doi.org/10.1007/s12209-015-2375-2

[33] H. Tan, D. Wang, Y. Guo, Materials **12**, 2279 (2019). DOI: http://dx.doi.org/10.3390/ma12142279

[34] F. Zhang, L. Cui, K. Lin, F. Jin, B. Wang, S. Shi, D. Yang, H. Wang, F. He, X. Chen, S. Cui, J. Alloys Compd. **553**, 367-374 (2013). DOI: http://dx.doi.org/10.1016/j.jallcom.2012.12.005

[35] Y. Zhou, N. Wang, J. Muhammad, D. Wang, Y. Duan, X. Zhang, X. Dong, Z. Zhang, Carbon **148**, 204-213 (2019). DOI: https://doi.org/10.1016/j.carbon.2019.03.034